



# Computational modeling of worker exposure scenarios during oil well logging

Tatiana M Tamura<sup>1</sup>, Arthur S B Z Alves<sup>3</sup>, Lucio P Neves<sup>2,3</sup>, Ana P Perini<sup>2,3</sup>,  
Carla J Santos<sup>3</sup>, Walmir Belinato<sup>4</sup>, Albérico B C Junior<sup>5</sup>, and William S Santos<sup>2,3</sup>

<sup>1</sup> Geography Institute, Federal University of Uberlândia (IG/UFU), Uberlândia, 38400-902, Brazil

<sup>2</sup> Physics Institute, Federal University of Uberlândia (INFIS/UFU), Uberlândia, 38408-100, Brazil

<sup>3</sup> Postgraduate Program in Biomedical Engineering (PPGEB/UFU), Electrical Engineering Faculty, Federal University of Uberlândia, Uberlândia, 38400-902, Brazil

<sup>4</sup> Federal Institute of Bahia (IFBA), Vitória da Conquista, 48030-220, Brazil

<sup>5</sup> Federal University of Sergipe (UFS), São Cristovão, 49107-230, Brazil

Correspondent author: arthur.zuchetti@ufu.br

**Abstract.** The use of ionizing radiation sources in the oil prospecting industry poses a challenge to workers and to radiological safety. During oil well logging procedures, workers are exposed to radiation emitted by radioactive sources used to obtain information on rock types, reservoir layer thicknesses, porosity, permeability, and others. Among several sources of ionizing radiation, <sup>241</sup>Am-Be is one of the most commonly used. The objective of this research is to develop computational exposure scenarios involving workers during the logging of oil wells with nuclear probes and to determine the radioactive doses that these individuals are exposed to. A set of conversion factors for equivalent and effective dose was calculated for the tube operator and the driver of the vehicle transporting the tube. The absorbed doses in the workers organs and tissues, and the fluence of particles around the oil well were determined using the radiation transport code MCNPX2.7.0. The exposed individuals were represented by computational anthropomorphic phantoms from ICRP 110 reference. Particle fluence maps were determined to characterize the radiation field, around the well, generated by the <sup>241</sup>Am-Be source. Considering an exposure time of 10 minutes and a typical activity of 333 GBq, an effective dose of 73 mSv for the operator was obtained, which is higher than the dose limit recommended by the ICRP of 20 mSv per year. Particle fluence maps showed that the most critical points for the workers were when the source is operated at the well entrance. Therefore, the results showed that neutron source handling must follow operational procedures, training, handling, regular verification of devices, and regulatory control.

## 1. Introduction

Oil is one of the main inputs in the energy matrix and is still irreplaceable in some applications such as fuels and petrochemical products. The production cycle begins with exploration, the objective of which is to find and quantify hydrocarbon reserves and extract them profitably. For this, promising geological formations for the formation and accumulation of oil are sought [1].

Oil deposits are available in nature in underground formations, and, through good drilling, profiling techniques become a tool that allows the interpretation of intervals, indicating the existence or not of hydrocarbons and allowing access to oil and gas.

Well logging involves geological data analysis studies and the geophysical methods application such as seismic prospecting, magnetometer, and gravimetry to identify rocks where oil may be stored. By providing information about formations, such as lithology (types of rock), the thickness of reservoir intervals, porosity, permeability, and saturation of fluids present, among others in its profiling, thus well profiling has been indispensable in oil exploration. In this context, the use of different types of radioactive sources involved in oil well logging poses a challenge to radiological safety. Among several existing sources, gamma radiation ( $^{137}\text{Cs}$ ) and neutron sources ( $^{241}\text{Am-Be}$ ) are the most used [1,2]. These sources are shielded and stored inside containers, and when they are used, their shielding is removed and transported by a steel cable system along the depth of the well to obtain information on lithological profiles and other data. Although knowing the benefit of using these sources, it is important to know how this procedure can influence the exposure of workers [3,4]. By this means, this research aims to evaluate the exposure of professionals involved during the oil well logging process and, therefore, provide dosimetric data, since there is a lack of information on this topic in the literature. To obtain the dosimetric values, Monte Carlo method and computational anthropomorphic phantoms were used.

## 2. Material and Methods

### 2.1. Development of the exposure computational model using the MCNPX2.7.0 code

The simulations were performed with the MCNPX2.7.0 radiation transport code, developed by the Los Alamos National Laboratory [5]. This code can simulate the particles radiation transport in different media, theoretically imitating statistical processes. Through this code, it is possible to model computational exposure scenarios for photons and 34 other types of particles, including neutrons, electrons, light ions, and more than 2000 heavy ions in a wide range of energies. In addition, MCNPX2.7.0 provides an extensive set of cross-section libraries and physical models.

### 2.2. Representation of exposed individuals

To determine the equivalent and effective doses that the probe operator and the driver of the probe transport vehicle would receive during the profiling process, the male and female computational anthropomorphic phantoms referenced in the publication ICRP 110 [6] were used in the postures of standing and sitting (Figure 1). These phantoms have all organs with dosimetric importance for calculating the effective dose recommended by ICRP 103 [7] and, consequently, were chosen for this study. Some of the information from these anthropomorphic phantoms is presented in Table 1.

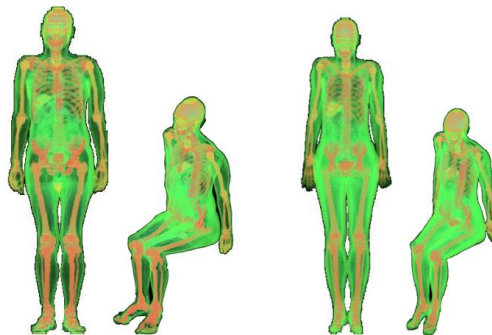


**Figure 1.** Male anthropomorphic phantoms in standing and sitting positions (left) and female in standing and sitting positions (right).

**Table 1.** Characteristics of the voxel matrix of the reference male and female anthropomorphic phantoms from the publication ICRP 110 [6].

Properties	Standing		Sitting	
	Male	Female	Male	Female
Height (m)	1,76	1,63	1,39	1,34
Mass (kg)	73,0	60,0	73,0	60,0
Z voxel dimension (mm)	8,0	4,84	2,0	1,16
X and Y voxel dimension (mm)	2,137	1,775	2,137	1,775
Voxel volume (mm <sup>3</sup> )	36,54	15,25	9,13	3,66
Number of voxels along the X axis	254	299	260	310
Number of voxels along the Y axis	127	137	370	370
Number of voxels along the Z axis	222	348	696	829

### 2.3. Modeling of the <sup>241</sup>Am-Be neutron source

The system to be analyzed in the logging process consists of a <sup>241</sup>Am-Be neutron source, positioned on the axis of a well located in a limestone formation. The neutron source is inside a metal casing distributed in a metal cylinder of 8.8 cm in diameter and 5.0 cm in length, containing an initial activity of 333 GBq (9 Ci) [8]. The power supply capsule provides shielding in all directions except the front. Aligned to the source are two detectors enriched with 95% <sup>6</sup>Li that provide neutron flux count information. The rig has a hollow cylinder designed to fit the logging tool that carries the source into the well. When not in use, the source assembly fits inside an armored storage container which is used for safe source storage and for transporting the source to well sites. Figure 2 shows a detailed view of the main components of the probe and source.

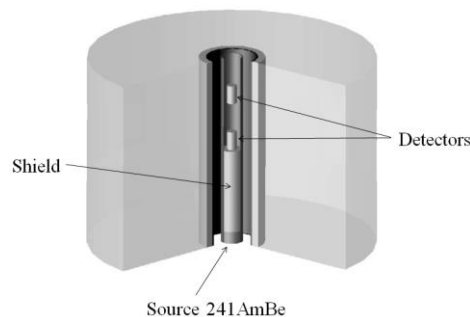


**Figure 2.** Schematic representation of the probe with neutron source (<sup>241</sup>Am-Be).

### 2.4. Modeling of the exposure computational scenario

Using the MCNPX2.7.0 code, a model of the main equipment for the profiling operation was defined, consisting of a vehicle for transporting the profiling unit, cable, and profiling probe. The vehicle has a container made of iron and zinc, with dimensions (530 x 240 x 200) cm<sup>3</sup> and the driver's cabin in iron measuring 120 x 250 x 170 cm<sup>3</sup> [9]. Figures 3A and 3B show a top and interior view of the rig transport vehicle, the oil well, the operator, and the main structures of the rig used in the logging process. The modeling of the vehicle carrying the probe was necessary for a more accurate assessment of the driver's exposure.

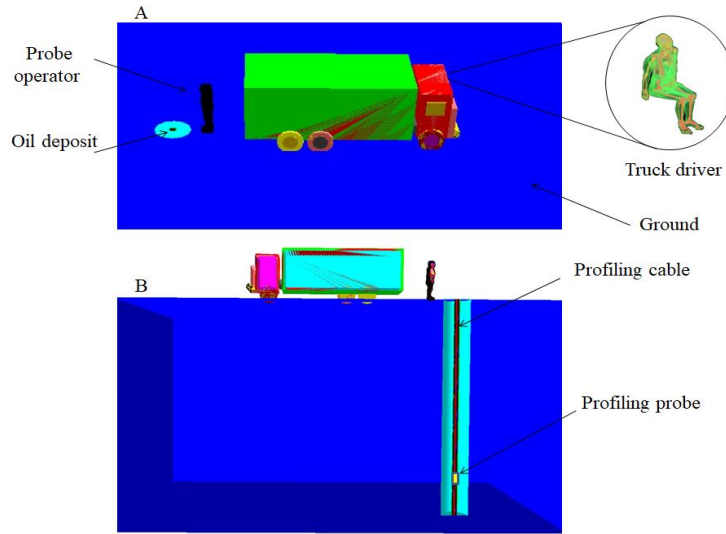


**Figure 3.** Oil well logging operation scheme: external (A) and internal (B) view of the logging unit.

### 2.5. Dosimetric calculations

The average deposited in each organ and tissue of the male and female anthropomorphic phantoms was determined using the F6 tally (MeV/g/particle) of the MCNPX2.7.0 code. The dosimetric evaluation presented by this study will be based on conversion factors (CF) for equivalent (H) and effective dose (E) normalized by the initial activity of the source in GBq.s. The neutron equivalent dose of organs and tissues was calculated using the card DF n iu=2 FAC=-3 ic=99 of each tally of code MCNPX2.7.0, which converts the absorbed neutron dose to the equivalent dose rate in Sv/h/source-particle. The simulated absorbed doses for photons were calculated using the tally F6 which gives the result of the deposited energy in MeV/g/particle. To convert this result to J/kg, it was multiplied by the conversion factor: 1 MeV/g = 1.602E-10 J/kg. The absorbed dose ( $D_T$ ) and equivalent dose ( $H_T$ ) were calculated using Equations 1 and 2 [10], respectively,

$$D_T = F6 \left( \frac{\text{MeV}}{\text{g}} \right) \times 1.602E - 10 \left( \frac{\text{J}}{\text{MeV}} \right) \quad (1)$$

$$H_T = \sum w_r \times D_T \quad (2)$$

where  $w_R$  is the radiation weighting factor, whose value for photon and electron is 1, and, therefore, in this case, the equivalent dose is equal to the absorbed dose. The calculation of the effective dose (E) was performed using Equation 3 [10].

$$E = \sum_T w_T \left[ \frac{H_T^F + H_T^M}{2} \right] \quad (3)$$

where  $H_T^F$  and  $H_T^M$  are the equivalent doses for the organs and tissues T of the female and male phantom, respectively,  $w_T$  is a tissue weighting factor derived from the relative radiosensitivity of each organ or tissue proposed by ICRP [10].

In addition to the set of FCs in terms of initial source activity, in this study, we present absolute dosimetric data for a hypothetical case using an initial source activity of 333 GBq (9 Ci).

To reduce the relative statistical errors associated with the dosimetric magnitude of organs and tissues, one billion particle histories were used in each scenario. All simulations were performed on a computer with 16 GB of RAM memory with a first-generation Intel Core i7 2.8 GHz processor and

Windows 7 64-bit operating system. Computational time depends on the amount of voxel in the anthropomorphic phantom but floats between 30 and 40 h.

### 3. Results e Discussion

In this study, the equivalent and effective doses of workers, female and male, involved in oil well logging activities using probes that operate with neutron sources ( $^{241}\text{Am-Be}$ ) were simultaneously determined. In the same computational exposure scenario, the rig operator and the driver of the vehicle that transports the rig to the profiling site were present. All irradiation scenarios were simulated with the MCNPX2.7.0 radiation transport code, which allows accurate modeling of complex geometries. The workers were represented by anatomically realistic anthropomorphic phantoms of ICRP 110 reference [6]. It is important to highlight that workers' exposures were evaluated only when the probe was positioned from the entrance to the well.

Conversion factors for equivalent and effective doses were calculated for source depths at the well entrance (0 cm), 40, and 60 cm. Due to the shielding generated by the earth layers and the distance from the source to the driver (approximately 8.0 m), the dosimetric results were accompanied by percentage relative errors that exceeded 50% for the depths of the source 40 and 60 cm and, for this reason, the vehicle driver dosimetric data were presented only for the source located at the well entrance (0 cm), where the generated errors were lower. The results for the vehicle driver and for the probe operator are presented in Table 2.

As can be seen in Table 2, the CFs drastically decreases with the distance from the worker to the source. In addition to the distance, the materials of the vehicle's structures contribute to the reduction of doses. Compared to the probe operator's dosimetric data, the driver obtained significantly lower values. As an example, for the source at the well entrance, the CF for effective dose calculated for the driver was  $7.8\text{E-}07$  mSv/GBq.s and for the rig operator it was  $3.7\text{E-}04$  mSv/GBq.s, that is, about 474 times higher than the driver. This behavior suggests that the exact determination of the workers' distances from the source is an important aspect in the calculation for a good dosimetric estimate. The results also show that the position of the organ in relation to the ground is an important factor. The male probe operator is 176 cm tall, and the female operator is 163 cm. The distance from the floor to the gonads and bladder of these individuals is about 90 cm. The distance from the source to these organs is approximately 135 cm, consequently, a smaller source-organ distance translates into greater exposure of organs close to the ground, mainly for the gonads of the male, which is an external organ and does not have natural shielding of the organs and organs. other body structures. Due to the lower distance of the organs from the ground, most organs of the female anthropomorphic phantom were more irradiated than the organs of the male anthropomorphic phantom. For both genders, another important aspect is the size and distribution of organs in the body, thus organs with larger volumes and distributed throughout the body, such as, for example, red marrow, bone surface, and stomach, were heavily irradiated.

The calculated organ doses are weighted by the tissue weighting factors used by the ICRP to obtain the effective dose, which is the amount evaluated for each worker, in this case. Table 2 presents the CFs for the effective dose for the probe operators and for the driver derived from the mean organs of the male and female anthropomorphic phantoms. As expected and proven, the highest results were calculated for the source at the well entrance (0 cm). In this case, there was no shielding generated by the earth layers and, therefore, the intensity of the radiation that reached the workers was greater. For all situations, the calculations show that the CFs decreases as the source depth in the well increases. Another important piece of information is that the calculations were performed assuming that the probe operators were exposed during the entire exposure period from the front of the body, which we believe is the most critical posture.

This study assumed a hypothetical case. The most critical exposure scenario for workers was considered, that is when the radiation source was positioned at the entrance to the well. In addition to this consideration, a typical source activity of 333 GBq (9 Ci) and 10 minutes of exposure was defined.

Applying these data to the results of the effective dose CFs for the vehicle driver and the probe operator (Table 2), we obtain the absolute effective dose values of 0.16 and 73 mSv for the vehicle driver and operator probe, respectively. To protect individuals against the harmful effects of exposure to ionizing radiation, the ICRP establishes a dose limit for occupationally exposed individuals (OEI), that is, for people who work with sources of ionizing radiation. For OEI, the annual effective dose is 20 mSv averaged over a defined period of 5 years (100 mSv over 5 years) with the proviso that the effective dose should not exceed 50 mSv in a single year. Therefore, the probe operator's effective dose value was higher than the dose limit recommended by the ICRP for occupational exposure. Therefore, the values of dosimetric results for professionals tend to increase with the increase in the number of work activities and, therefore, this study recommends the adoption of additional radiological protection care to ensure that the dose limits are not exceeded.

In this study, the mesh tally card code MCNPX2.7.0 was used to determine the neutron fluence (in MeV/cm<sup>3</sup>/particle) on the soil surface for the source at the well entrance and 60cm deep in the oil well. The results for depths 0 cm and 60 cm are shown in Figures 3A and 3B, respectively.

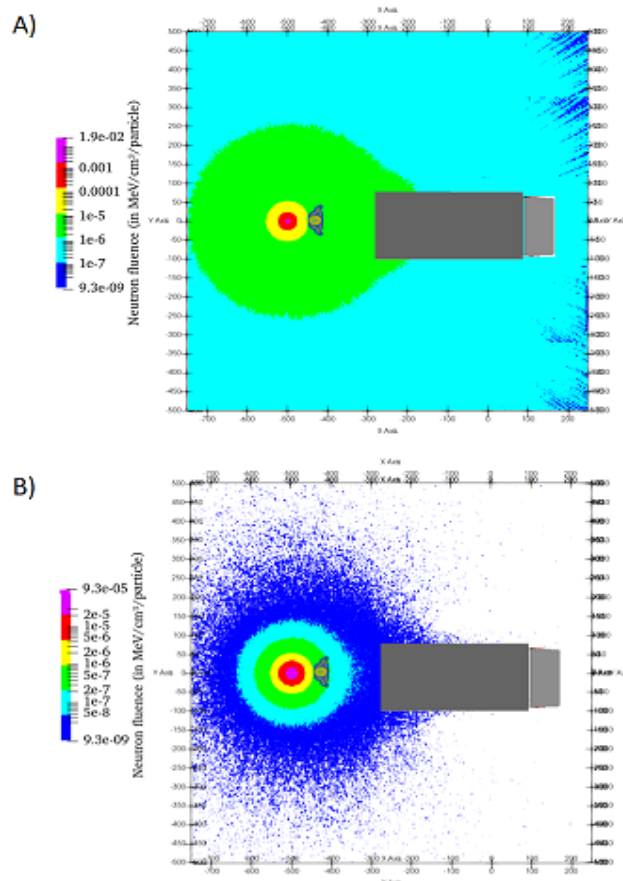


**Figure 3.** Particle fluence on the soil surface with the source located at the well entrance (Figure 3A) and at a depth of 60 cm (Figure 3B).

It can be seen that, the intensity of the radiation decreases as the depth of the source increases. Due to the natural shielding generated by the earth layers and the distance between the driver and the well, this worker's exposure was lower among the evaluated professionals. A different scenario was found for the rig operator, as this was only 1 m from the well contour and, therefore, was the most irradiated professional.

**Table 2.** Conversion coefficients for equivalent dose normalized by the absorbed dose in air (in mSv/GBq.s) as a function of source depth in the oil well. In parentheses are the percentage relative errors.

Organ	Probe operator						Vehicle driver	
	0 cm		40 cm		60 cm		0 cm	
	Male	Female	Male	Female	Male	Female	Male	Female
Stomach	2.5E-04 (0.6)	3.8E-04 (0.6)	2.6E-05 (1.3)	4.0E-05 (1.3)	7.2E-06 (2.3)	1.1E-05 (2.4)	1.7E-07 (6.8)	1.8E-07 (5.9)
Colon	7.3E-05 (0.3)	1.1E-04 (0.3)	7.3E-06 (0.8)	1.1E-05 (0.8)	2.0E-06 (1.3)	3.1E-06 (1.3)	6.8E-07 (4.0)	9.4E-07 (3.8)
Liver	2.0E-04 (0.3)	3.1E-04 (0.3)	2.0E-05 (0.6)	3.2E-05 (0.7)	5.7E-06 (1.1)	8.9E-06 (1.2)	3.4E-07 (3.2)	4.9E-07 (3.3)
Lungs	1.9E-05 (0.3)	3.1E-05 (0.3)	1.9E-06 (0.7)	3.1E-06 (0.7)	5.3E-07 (1.3)	8.9E-07 (1.3)	8.8E-07 (15)	1.0E-06 (16)
Esophagus	1.3E-04 (1.3)	2.0E-04 (1.3)	1.3E-05 (3.1)	2.0E-05 (3.1)	3.8E-06 (5.5)	5.0E-06 (5.6)	1.7E-06 (3.6)	2.1E-06 (3.6)
Brain	1.0E-04 (0.4)	1.8E-04 (0.4)	1.3E-05 (0.9)	2.5E-05 (0.8)	3.8E-06 (1.5)	7.4E-06 (1.4)	3.6E-06 (1.3)	2.2E-06 (1.5)
Red marrow	2.0E-03 (0.1)	1.5E-03 (0.1)	1.2E-04 (0.2)	9.8E-05 (0.2)	3.4E-05 (0.4)	2.8E-05 (0.4)	1.0E-06 (20)	1.5E-06 (22)
Thyroid	2.2E-04 (1.7)	3.8E-04 (1.7)	2.0E-05 (3.7)	4.4E-05 (3.7)	8.1E-06 (6.2)	1.5E-05 (6.2)	8.3E-07 (18)	4.9E-07 (35)
Gonads	4.0E-04 (0.8)	2.1E-04 (1.7)	3.6E-05 (1.9)	1.5E-05 (4.5)	1.1E-05 (3.3)	3.7E-06 (8.2)	3.1E-07 (16)	4.9E-07 (18)
Bladder	4.1E-04 (0.7)	7.4E-04 (0.6)	3.3E-05 (1.8)	7.0E-05 (1.6)	8.3E-06 (3.2)	1.9E-05 (2.8)	1.3E-06 (1.3)	1.6E-06 (1.5)
Bone surface	7.1E-04 (0.1)	1.1E-03 (0.1)	4.2E-05 (0.2)	7.2E-05 (0.2)	1.2E-05 (0.4)	2.1E-05 (0.4)	1.0E-07 (0.8)	9.7E-08 (1.0)
Remain tissue	1.2E-05 (0.1)	1.5E-05 (0.1)	8.6E-07 (0.1)	1.1E-06 (0.2)	2.5E-07 (0.3)	3.2E-07 (0.3)	2.7E-06 (8.4)	2.1E-06 (10)
Salivary Glands	1.7E-04 (0.8)	2.2E-04 (0.9)	2.6E-05 (1.6)	3.4E-05 (1.6)	7.5E-06 (2.7)	1.0E-05 (2.8)	1.7E-06 (1.1)	1.8E-06 (1.2)
Skin	1.2E-04 (0.1)	1.6E-04 (0.1)	9.5E-06 (0.2)	1.3E-05 (0.2)	2.9E-06 (0.4)	4.0E-06 (0.4)	9.9E-07 (17)	8.1E-07 (4.8)
Breast	1.4E-04 (1.1)	1.6E-04 (0.4)	2.0E-05 (2.2)	2.3E-05 (0.7)	5.8E-06 (3.7)	6.8E-06 (1.2)	5.9E-07 (9.7)	8.3E-07 (7.7)
Effective dose	3.7E-04 (0.1)		2.9E-05 (1.3)		8.4E-06 (2.3)		7.8E-07 (8.7)	

#### 4. Conclusion

In this study, Monte Carlo simulations were used to model a computational exposure scenario for professionals involved in oil well logging using a neutron source probe ( $^{241}\text{Am-Be}$ ). The MCNPX2.7.0 radiation transport code and a pair of anthropomorphic phantoms, of both genders, were used to represent the probe operator and the vehicle driver. Workers' exposures to different source depths in the oil well were evaluated. The best results were obtained when the  $^{241}\text{Am-Be}$  source was at the well entrance and, therefore, it was considered the most critical scenario. Particle fluence curves show that the intensity of radiation decreases as you move away from the epicenter. For this reason, the probe operator was the most irradiated.

Considering the most critical scenario, an initial source activity of 333GBq and an exposure time of 10 minutes, it was concluded that the most irradiated organs were the red marrow (0.73 mSv/male), salivary glands (0.54 mSv/male) and skin (0.36 mSv/female). For the probe operator, the most irradiated organs were the red marrow (390 mSv/male), bone surface (220 mSv/female), and bladder (150 mSv/female). Due to the closer relative distances of the organs to the ground and the source, the organs and tissues of the female anthropomorphic phantom were the most irradiated and, consequently, contributed to the increase in the effective dose, whose results were 73 and 0.16 mSv for the probe operator and the vehicle driver, respectively. The effective dose result for a single exposure of the probe operator showed that additional care is needed, as it exceeded the dose threshold for occupational exposure and tends to be more critical with the increase in the number of work activities and exposure time.

#### 5. References

- [1] IAEA. International Atomic Energy Agency Radiation protection and the management of radioactive waste in the oil and gas industry. IAEA. Safety Reports Series n°. 34, 2003.
- [2] UNSCEAR. United Nations Scientific Committee on the Effects of Atomic. Sources and effect of ionizing radiation. Unsear, report to the general Assembly with scientific Annex v. 2; 2008.
- [3] Amidu, M. A, Appah, T, Adewale, D. Risk Assessment of Abandoned radioactive logging sources in oil wells in Nigeria. J. Environ. Earth Sci. v. 3, n° 10, 2013.
- [4] Bello, N.A. Regulatory framework for safety and security of radioactive sources used in nuclear well logging, presented at the 1-day technical meeting on the abandonment of radioactive sources stuck in oil wells, 2007.
- [5] Pelowitz, D.B. MCNPX User's Manual, version 2.7.0. Report LA-CP-11-00438. Los Alamos National Laboratory, 2011.
- [6] ICRP 110. International Commission on Radiological Protection Publication 110. Adult reference computational phantoms. Ann. ICRP 39, Oxford: Elsevier, 2009.
- [7] ICRP 103. International Commission on Radiological Protection. Recommendations of the ICRP publication 103. Elsevier, v. 37, p. 61-62, 2007.
- [8] Strub, T., Van, T., Gregory J. Large Radiological Source Production and Utilization and Implications Regarding RDDs, Los Alamos National Laboratory Report LA-UR-03-5432, July 2003.
- [9] CEI-IEC. Installed monitors for the control and detection of gamma radiations contained in recyclable or non-recyclable materials transported by vehicles. International Standard CEI IEC 62244. Geneva, Switzerland, 2006.
- [10] ICRP 116. Conversion coefficients for radiological protection quantities for external radiation exposures. Publication 116. Ann., v. 40, p. 2 – 5, 2010.

#### Acknowledgment

The authors thank the grants CNPq 312124/2021-0 (APP), 314520/2020-1 (LPN), 309675/2021-9 (WSS), UNIVERSAL CNPq 407493/2021-2 (APP, LPN and WSS), 40303/2022-3 (APP, LPN and WSS); and FAPEMIG APQ-04215-22 (APP).